Available online at www.sciencedirect.com

ScienceDirect

Publishing Services by Elsevier

International Journal of Naval Architecture and Ocean Engineering 10 (2018) 348–359
http://www.journals.elsevier.com/international-journal-of-naval-architecture-and-ocean-engineering/

Experimental investigations on seismic response of riser in touchdown zone

Yunyun Dai, Jing Zhou*

State Key Laboratory of Coastal and Offshore Engineering, Dalian University of Technology, No. 2 Linggong Road, Ganjingzi District, Dalian, Liaoning Province, 116024, PR China

Received 30 March 2017; revised 23 June 2017; accepted 15 August 2017
Available online 19 October 2017

Abstract

A series of indoor simulation tests on a large-sized shaking table was performed, which was used to simulate the earthquake ground motion for the pipe–soil interaction system to be tested. The purpose of this study is to examine the dynamic characteristic and seismic response of a length of PVC pipeline lay on a clay seabed under seismic load. The pipeline was fully instrumented to provide strain and acceleration responses in both transverse and in-line. Dynamical modal tests show that corresponding mode shapes vertically and horizontally are basically the same. But the absolute values of the natural frequencies vertically are all higher than those corresponding values in transverse. It turned out that the geometry configuration of riser affects its stiffness. Seismic response of pipeline depends significantly on the waveform, and Peak Ground Acceleration (PGA). As the seismic loading progressed, the strain response was severe around both TDZ and catenary zone. Additionally, strain responses in top and bottom positions were more severe than the result in left or right side of the pipeline in the same section.

Keywords: Steel catenary riser; Touchdown zone; 3D experiments; Modal analysis; Seismic response

1. Introduction

With the development of offshore oil fields to the deep sea environment, Steel Catenary Riser (SCR), connecting Floating Platform System (FPS) and subsea pipeline on the seabed, becomes an important structure (Park et al., 2016). It consists of catenary zone, touchdown zone and surface zone (Bridge et al., 2003). The critical point when the catenary riser firstly contact the seabed is the Touchdown Point (TDP). The area where the riser interacts with the seabed in deep sea environment becomes the Touchdown Zone (TDZ), as shown in Fig. 1. The structure is relatively flexible compared with the fixed offshore platform. The riser in service operates in the ocean for a long time and is subjected to complex work and environmental loadings, including ocean wave, current, inner pressure, outer pressure and also earthquakes. Besides, most of oil/gas field in South China Sea are in the Circum Pacific seismic belt, the most active seismic zone in the world (Duan et al., 2010). This greatly reduces the service life of the riser in TDZ, so the impact of earthquake would be very significant. Seabed of soft clay is usually generated in deepwater oil and gas field in South China Sea (Zheng et al., 2004). Earthquake action on the seabed could induce a complex interaction process of pipeline and soil in TDZ (Arifin et al., 2010; Elosta et al., 2013; Yu et al., 2013, 2015). In this extreme condition, resistance and suction effect of the seabed on the pipeline in TDZ may cause an increase in the local riser stresses and strains (Madani et al., 2015).

Many researches have focused on examining the interaction mechanics of pipe and soil (Bridge et al., 2003; Hodder and Byrne, 2010; Wang et al., 2013, 2014; Ryu et al., 2015; Yu et al., 2017). Main techniques for investigating TDZ include numerical analysis method and experimental method. A variety of assumptions were put forward by scholars for exploring the dynamic behaviour of riser in TDZ. Bai et al. (2015) established the finite element contact model of riser and soil

* Corresponding author.
E-mail address: zhouj@dlut.edu.cn (J. Zhou).
Peer review under responsibility of Society of Naval Architects of Korea.

http://dx.doi.org/10.1016/j.ijnaoe.2017.08.005

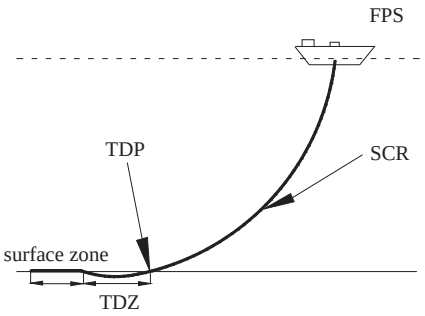

Fig. 1. Sketch of SCR in touchdown zone.

spring by using the equivalent spring element based on pipeline large deflection curve and the theory of elastic beam. Hawlader et al. (2016) proposed a numerical model to simulate suction and trench formation at the TDZ of SCR. Hejazi and Kimiaei (2016) developed a simplified equivalent linear soil stiffness formula in fatigue design of SCR based on the studied parameters based on the nonlinear results. Dai and Zhou (2016) proposed a solid-spring model to explore the dynamic characteristics of pipeline in TDZ and revealed dynamic response of some feature points. Kim et al. (2017) investigated the fatigue performance of touchdown zone based on a nonlinear soil model through time domain approach. Whereas, the effect of earthquake on dynamic behaviour of riser in TDZ have not been investigated. In experimental study of pipe–soil interaction, Bridge et al. (2003), Hodder and Byrne (2010), Wang et al. (2014) have conducted full-scale test and laboratory scale model test of pipe–soil interaction in TDZ. Their previous work on the interaction mechanism of pipe and soil laid a foundation for the numerical model assessment and validation. However, their researches just modelled the riser from surface zone to touchdown zone, ignoring the catenary zone. Moreover, seismic loading has not been considered, either.

When the pipe–soil system in service is subjected to earthquake, the seismic response of pipeline in TDZ is much more complex (Wu et al., 2016), becoming a challenging academic and engineering problem in offshore engineering. Merifield et al. (2009) examined partially embedment of pipelines on seabed due to the traction of the platform vertically. Elosta et al. (2013) invested SCR–seabed interaction in non-linear time domain based on the commercial code OrcaFlex. Quéau et al. (2014) studies the static stress range and its dynamic amplification factors of TDZ under oscillating loading. Hawlader et al. (2015) developed two different numerical modelling techniques, finite element and finite volume methods, to simulate riser-seabed-water interaction near the touchdown zone. Quéau et al. (2015a,b) have approximately researched the maximum stress range in the TDZ using several artificial neural networks for accessing the fatigue life of selected example SCRs. And Quéau et al. (2015a,b) explores the sensitivity of the maximum dynamic stress ranges and dynamic amplification factor (DAF) to the key dimensionless groups of input parameters and also certain individual input parameters. Firoozabad et al. (2016) proposed a failure criterion for steel pipe elbows with small curvature under cyclic loading. Although a number of models and research papers related to static load or static cyclic load have been published, there have been few reports on the seismic response of pipeline in TDZ (Arifin et al., 2010; Won et al., 2015). And most of the seismic research remains in the stage of numerical analysis.

Therefore, it is really necessary to develop better understanding of the seismic response in the TDZ when the pipe–soil system is subjected to earthquake. Both Hodder and Byrne (2010) and Wang et al. (2014) have respectively conducted lab-scale tests of pipeline from surface zone to touchdown zone by using PVC and PE material for their low material stiffness. The test in this paper focused on the seismic response of riser in TDZ, so the pipeline model of PVC was extended from surface zone to touchdown zone to catenary zone. A lab-scale seismic test program of pipeline in TDZ was adopted to examine the dynamic characteristics and seismic response of pipeline. The objective was to assess the dynamic characteristic of structure and seismic response along pipeline and pipe ring in earthquake, and to explore some critical factors in affecting the seismic response.

2. Test instrument

2.1. Pipe–soil interaction model

The lab-scale SCR model lay on the consolidated clay tank fixed on the shaking table subjected to earthquake was simulated as shown in Fig. 2. The first attempt was to observe the dynamic characteristics and mode shapes of the pipeline-soil system in this state. And the second objective was to detect dynamic time history response and spectral response of the pipeline under different seismic loadings. However, in view of the laboratory measurements and the execution conditions, it's unfeasible to simulate the whole scale of the SCR. So a reduced PVC pipeline model is manufactured due to the size and excitation parameter of the shaking table, whose geometric dimensions and excitation parameters are shown in Fig. 3 and Table 1. Thus, some properties of the PVC model pipeline and seabed consolidated by soft clay, such as diameter and additional mass of pipeline, and consolidation pressure of seabed, needed to be manufactured to accommodate the model scale.

2.2. Consolidated seabed

The model seabed in the present study was consolidated by a type of soft red clay, which was taken from a foundation pit in Dalian. With the purpose of in keeping with the soil properties in South China Sea (Zheng et al., 2004), the sample seabed preparation process contained five steps. Firstly, a metal flume with drainage valves (2 mm diameter) on the bottom was manufactured, whose size is 3 m long, 1 m wide, 0.6 m high. Secondly, cover the bottom of the flume with 60 mm thick gravel drainage layer; then place a sheet of geotextiles on the top of the drainage layer; then place a sheet

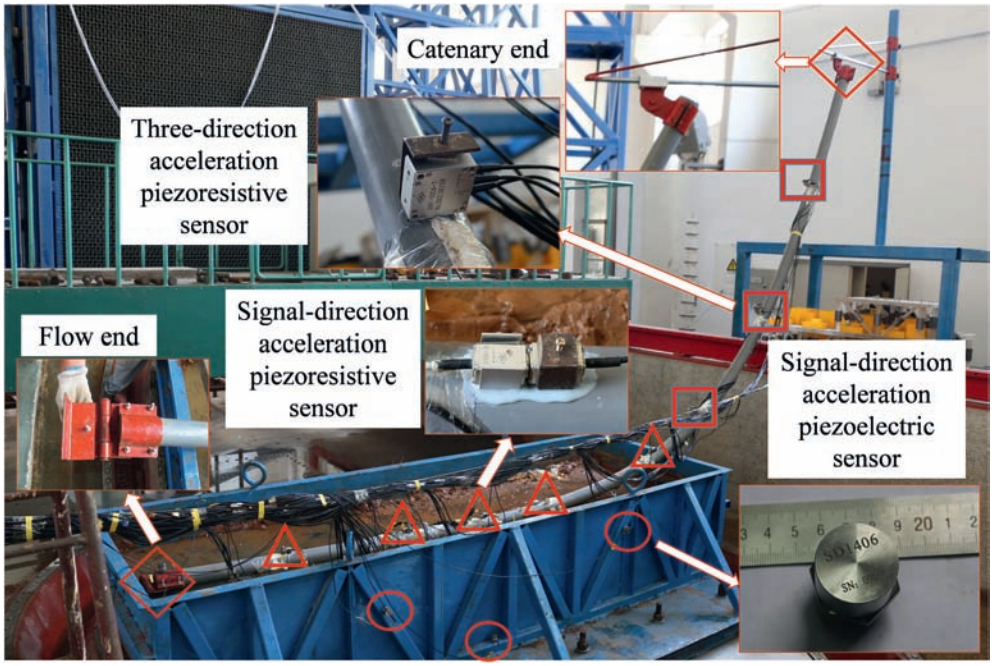

Fig. 2. Overall view of the large scale 3D system pipe–soil system.

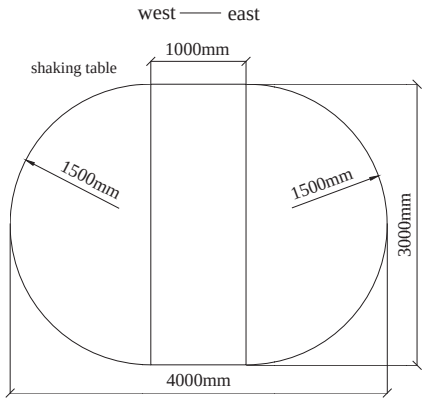

Fig. 3. Plane graph of the shaking table.

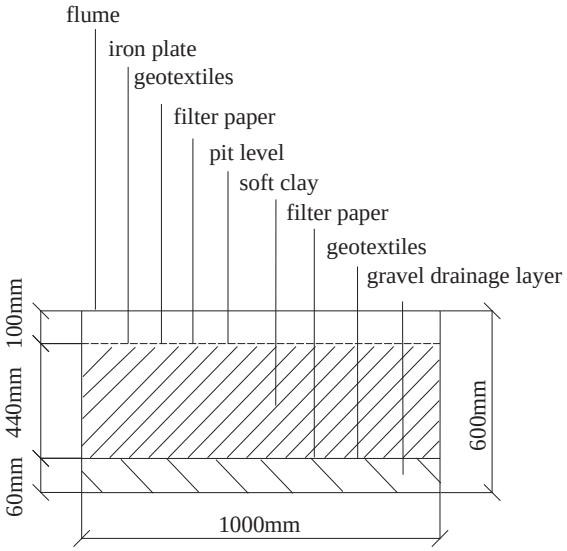

Fig. 4. Cross-section of the seabed in flume.

of filter paper, shown in Fig. 4. Thirdly, in order to remove large particles and the impurities, the red clay was sieved in water by a sifter (2 mm sieve pore). Subsequently, pour the fabricated slurry into the metal flume carefully and the soil surface was manually smoothed. Fourthly, the seabed was consolidated under self-weight in the first 10 days. Then cover the filter paper, the geotextiles, and iron plate in sequence for pressure consolidation. Finally, the seabed was consolidated under different increasing levels of pressure. The final pressure was up to 27.77 kPa. During the whole process of consolidation, soil settlements in four points were monitored and recorded. After about 1 month, the gradient consolidation test completed and then the subsequent tests were carried out. The average soil thickness after consolidation was about 450 mm (>4D), which is adequately deep for neglecting bottom boundary effects (Wang et al., 2014). Similarly, the side boundary effects can also be ignored due to the width (7.5D) of the model seabed (Wang et al., 2014). The flume was made up of stiffened steel plate, and then fixed on the shaking table,

Table 1
The actuator parameters of the shaking table.

Parameter	Vertical	Lateral
Maximum displacement (mm)	±50	±75
Maximum velocity (cm/s)	35	50
Maximum acceleration (g)	0.7	1.0
Maximum load mass (kg)	10,000	
Frequency (Hz)	0.1–50	

as shown in Fig. 2. Therefore, seabed model in this study can be considered a rigid boundary condition.

Key geotechnical parameters of soil and seabed listed in Table 2 were obtained from a series of tests on the red clay sample and consolidated seabed. Both liquid limit and plastic limit were obtained from combined measurement test of liquid and plastic limits test on the red clay. Liquid limit means the critical moisture content of red clay between liquid to plastic states. Similarly, plastic limit is the critical moisture content of clay between plastic to solid states. As shown in Table 2, liquid and plastic limits are 41.3 and 17.7, respectively. And the plastic index (PI) is the relative moisture content of liquid and plastic limits. Its value is 23.6. Undrained shear strength of the seabed, obtained from T-bar test, is 4.58 kPa, which is popular along the South China Sea (Zheng et al., 2004). It can represent the main phenomena involved in pipe soil interaction usually encountered in the deepwater environment of South China Sea.

2.3. Pipeline

As an experiment with a truncated model could be more precise and easier to carry out, the aim of this research was a global evaluation of the SCR in TDZ. In order to keep the structural properties, such as structure modal and dynamic response as close as possible to the TDZ prototype, a reduced PVC model pipeline (6 m long, 75 mm diameter, 2.3 mm thick) was selected on account of its low material stiffness and a relatively larger diameter, which allowed the demands of pipeline deformation from surface zone to TDZ, to catenary zone. Furthermore, the larger diameter also met the instruments installation. Due to the motion of the floating facility, will result in cyclic rotations and horizontal displacements at some location above the seabed (Hodder and Byrne, 2010), the top end of the pipeline in this test was hinged to an axial sliding point, shown in right side of Fig. 3, simulating a truncation from the whole riser. It could rotate in and out of the riser plane. The surface end of pipeline was hinged to anchor point on the flume, shown in left side of Fig. 3, simulating a truncation from the subsea pipeline in the surface zone. Some parameters of the reduced PVC model pipe such as stiffness, structure size, and mass were chosen and readjusted, shown in Table 3. In order to meet the requirements of structure mass, the actual lab-scale PVC model was equipped by 36 equally distributed inner solid cylinder of lead lumps (70.2 mm outer diameter, 15.8 mm inner diameter, 65 mm high), shown in Table 3 and in Fig. 5. The added mass was comprehensively determined based on the scale of shaking table, geometry and mechanical properties of PVC pipeline.

2.4. Arrangement of instrumentations and digital data acquisition system

The pipeline was fully instrumented to provide strain and acceleration responses in both transverse and in-line of the measure sections along its length. Three main kinds of sensors, strain gauge, piezoresistive accelerometers, and piezoelectric accelerometer, were installed in ten critical sections of the pipeline. The arrangement of the instrumentation is shown in Fig. 5. The strain gauges (model: BX120-3AA) were mounted axially and circumferentially in orthogonal phases of every section to measure the strain response in every point, shown in Fig. 5(b). Each strain gauge was equipped with a temperature compensation strain gauge, mounted on the surface of a segment of PVC pipeline with same type. In order to prevent water ingress leading to short-circuit during testing, a type of silicone rubber was covered on the strain gauge and wire to provide mechanical protection and insulation protection, shown in Fig. 6. The strain was recorded by the NI dynamic data acquisition system, and the sample frequency was 1700 Hz. Signal-direction (model: ARH-A, measuring range: 5 g, frequency response range: 0–120 Hz) and three-direction waterproof piezoresistive accelerometers (model: ARF-100A-T, measuring range: 10 g, frequency response range: 0–120 Hz) were used to detect the acceleration response of the riser in every section, including transverse and in-line direction. The accelerations of the shaking table horizontally and vertically were also recorded. The signal-direction piezoelectric accelerometers were installed on the mental flume. Accelerations were collected by the digital data acquisition system of the mobile data recorder (MDR), the sample frequency was 512 Hz.

Table 2
Geotechnical parameters of soil and consolidated seabed.

Physical properties	Liquid limit (%)	Plastic limit (%)	Plasticity index	Liquidity index Il	Water content (%)	Void ratio	Natural density (g/cm^3)	Unit weight (kN/m^3)	Modulus of compression Es (MPa)	Shearing strength S_u (kPa)
Value	41.3	17.7	23.6	2.34	43.604	1.4308	1.938	18.99	0.528	4.58

Table 3
Model parameters of PVC pipeline.

Parameter	PVC pipeline					Additional weight by lead lump			
	Outer diameter D_m/mm	Wall thickness t_m/mm	Length L_m/m	Young's modulus E_m/GPa	Density ρ_m/kg/m^3	Height h_{add}/mm	Outer diameter d_1/mm	Inner diameter d_2/mm	Number per unit length
Value	75	2.3	6	3.12	3.14E + 04	65	70.2	15.8	6

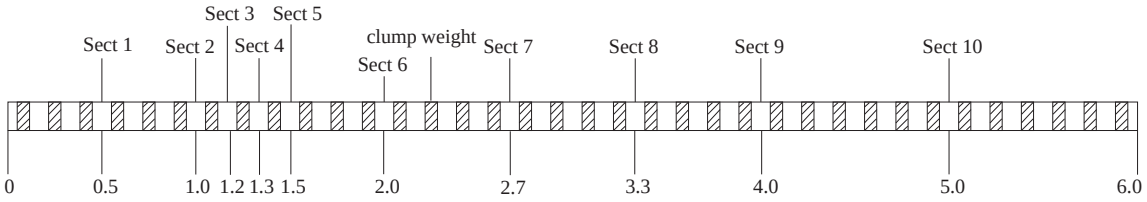

(a) Sketch of the model pipeline and section locations of instrumentations

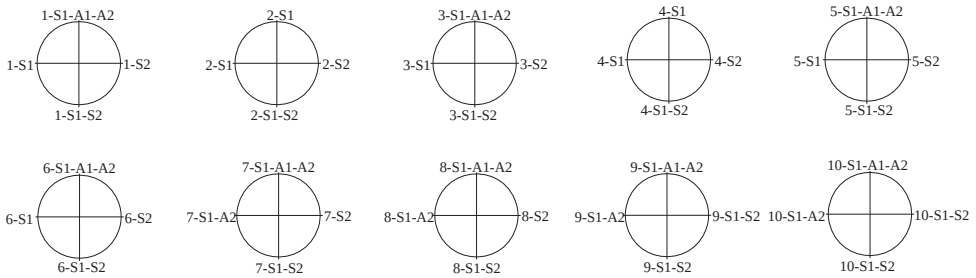

Serial number from 1 to 10 represents section number along the pipeline

S1——Axial strain sensor; S2——Circular strain sensor; A1——Transverse accelerometer; A2——In-line accelerometer.

(b) Instrumentations in every sectional view

Fig. 5. Distribution of instrumentations.

(a) Strain gage (b) Water repellent treatment

Fig. 6. Instrumentations processing and installation.

3. Test procedure

This test aimed to detect seismic response of riser in touchdown zone. Dynamic characteristics of the structure and dynamic responses of pipeline in different positions should be investigated clearly. Therefore, the whole test process contains two parts: first, modal test on the pipe–soil interaction model; second, dynamic response of the subsea pipeline subjected to seismic loading, including artificial sinusoidal wave excitation and random wave excitation.

3.1. Modal test

A set of pseudo white noise excitation experiments was conducted as modal tests of the pipe–soil structure system vertically and transversely. Natural frequencies and mode shapes are deserved from the modal tests. The operating conditions of pseudo white noise excitation tests are listed in Table 4.

Table 4
Cases of seismic test.

Group	Waveform	PGA (g)	Exaction frequency (Hz)	Sample frequency (Hz)
1	Sinusoidal excitation	0.1	3.32	1.7k
2	vertically	0.2	3.32	1.7k
3		0.5	3.32	1.7k
4	El-centro vertically	0.1		1.7k

3.2. Seismic test

In this article, a series of seismic loadings were subjected to the pipe–soil interaction system. Two earthquake waves, including artificial sinusoidal wave, and random El-centro waves were selected in this study. Its time duration and time interval were about 35 s and 0.0128 s, respectively. And with the purpose of fair comparison, their peak accelerations are adjusted from 0.1 g to 0.2 g, to 0.5 g. Details of waveform, amplitude, direction and frequency of seismic loadings are listed in Table 4 and in Fig. 7. This test was performed to investigate the dynamic response of the pipeline in different positions along pipeline.

4. Test result and interpretation

4.1. Modal test

4.1.1. Nature frequencies

Fig. 8 presents the strain response of section 10 in left side ($d = 5$ m) under pseudo white noise excitation (impact loading). It can be seen that the strain decayed gradually to stable equilibrium position in Fig. 8(a). Corresponding strain response spectrum is shown in Fig. 8(b), peak values and corresponding frequencies of first three orders could be obtained. The fundamental frequency, second-order frequency, third-order frequency of pipeline are 1.038 Hz, 3.11 Hz and 5.91 Hz.

Similarly, first three natural frequencies vertically could also be obtained by the modal test. Fig. 9 shows time history and response spectrum of strain just above section 10. The first three frequency values of pipeline vertically were 3.323 Hz, 7.89 Hz and 13.599 Hz respectively.

Comparison of natural frequencies of pipeline vertically and transversely from test analysis was also conducted, shown in Fig. 10. The absolute values of the natural frequencies vertically seemed higher than those corresponding values transversely. It turned out that the geometry configuration of riser affects its stiffness. It becomes stiffer vertically by reason of the geometrical configuration of pipeline in TDZ.

4.1.2. Mode shapes

Fig. 11 gives the first three order mode shapes transversely and vertically. On the whole, the corresponding normalised mode shapes transversely and vertically are basically the same, one peak in the first mode shape, one trough and one peak in the second mode shape, one trough and two peaks in the third mode shape. But there are some differences around TDZ between these two directions. Results vertically show a significant fluctuating phenomenon in TDZ. This was caused by the complex interaction mechanism of pipe and soil. The main reason is that the percussion test vertically will cause the pipeline to vibrate in some extent, which leads to cyclically contact and separation with the seabed. In the different state of contact and separation, constraints from seabed changes alternatively. Thus there will be a small fluctuation around TDZ. In transverse, the constraints from seabed in both sides are symmetrical, so the result in transverse seemed smoother.

4.2. Artificial sinusoidal wave excitation

4.2.1. Strain response along pipeline

To explore the effect of earthquake on the pipeline, Fig. 12 shows time history of strains of ten measured sections above when the pipe–soil system was subjected to sinusoidal excitation vertically, whose excitation frequency and peak value were 3.11 Hz and 0.1 g, respectively. Fig. 12(a) shows the whole process of strain responses in top of these ten sections ($\psi = 0°$) under this artificial sinusoidal wave excitation vertically. During the first 2 s of the earthquake, the strain response in every section begun to increase. This phenomenon was revealed clearly in a detailed figure with partial time scale in Fig. 12(b). When the strain response reaches its maximum firstly, it would decline then rise during the initial period of earthquake. It presented a phenomenon called “beat” from 2 s to 18 s. Then time history of strain entered into a steady state gradually from 18 s to 35 s. After the earthquake stopped, the strain response showed a trend of logarithmic decrement around its equilibrium position. It's worth noting that, in the beginning, the equilibrium position of every point was zero. However, after the earthquake, the equilibrium position in

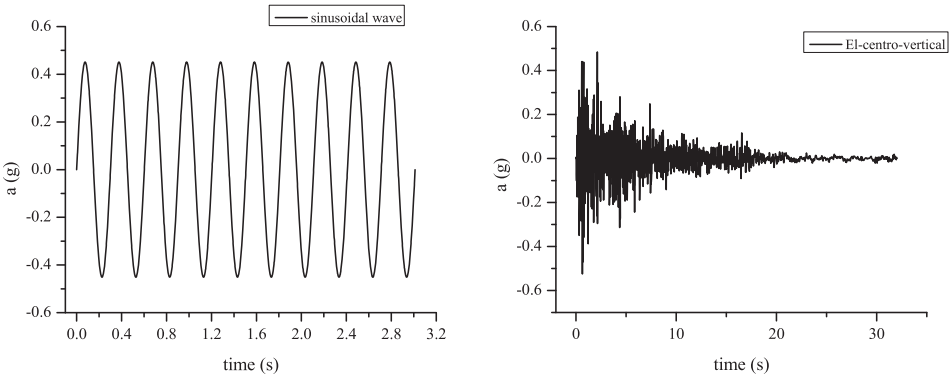

（a） Artificial sinusoidal wave excitation （b） El-centro wave excitation

Fig. 7. Time-history of two earthquake waves excitation.

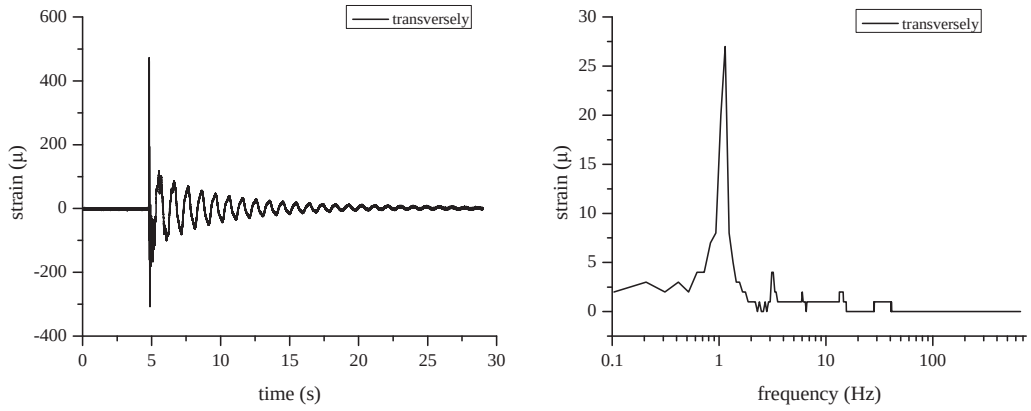

(a) Time history of strain response (b) Strain response spectrum

Fig. 8. Dynamic response of section 10 in left side under pseudo white noise excitation.

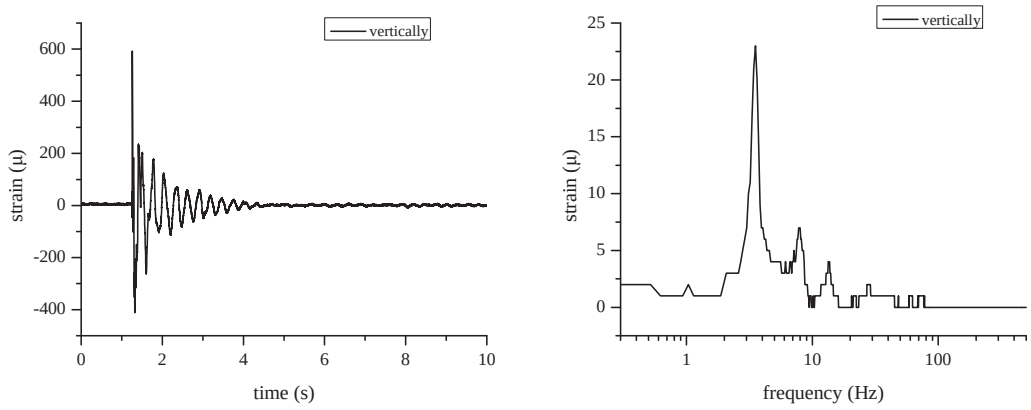

(a) Time history of strain response (b) Strain response spectrum

Fig. 9. Dynamic response of section 10 above under pseudo white noise excitation.

different position drifted away from zero in different extend. As we known, during the earthquake, pipe–soil interaction procedure was accompanied by seabed soil deformation and its performance degradation. The deformation of soil brought about the changes of pipe penetration and configuration, resulting permanent deformation. This can be used to explain the aforementioned test results.

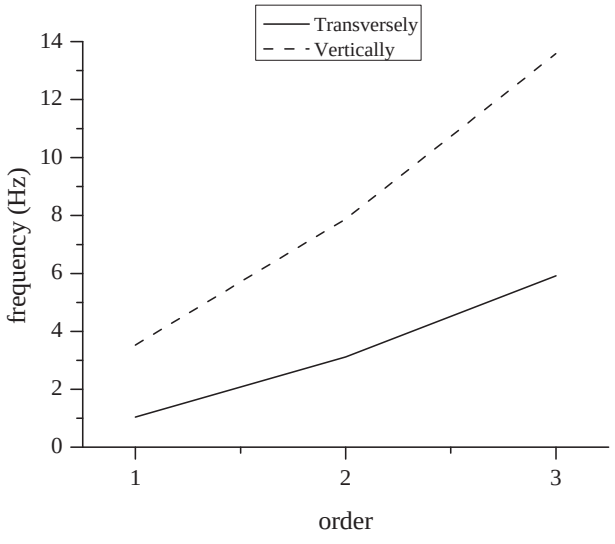

Fig. 10. Natural frequencies comparison transversely and vertically.

Seismic response of the pipeline in different positions along the pipeline presents different features. Fig. 13 presents time history of strain response in some special sections separately in the same time and strain scale.

Section $d = 0.5$ m – Pipeline in this location is in contact with the seabed soil, indicating the pipeline in surface zone, during the earthquake. Due to the constraints from the seabed, strain response in this section is very small, whose amplitude was not more than 50 micro-strain, as shown in Fig. 13(a).

Section $d = 1.0$ m – The edge of the TDZ, linked horizontal segment of the pipeline, also in contact with the seabed soil. Strain response in this section increased rapidly to magnitude of 400 micro-strain, as shown in Fig. 13(b).

Section $d = 1.5$ m – This location is in contact with the seabed for whole procedure of the seismic test. Time history of strain there, shown in Fig. 13(c), is mainly assisted by tension, like a down comb. This suggests soil resistance played a major role in this segment during earthquake.

Section $d = 2.0$ m – Another edge of the TDZ in contact with the seabed, linked catenary segment of the pipeline. It

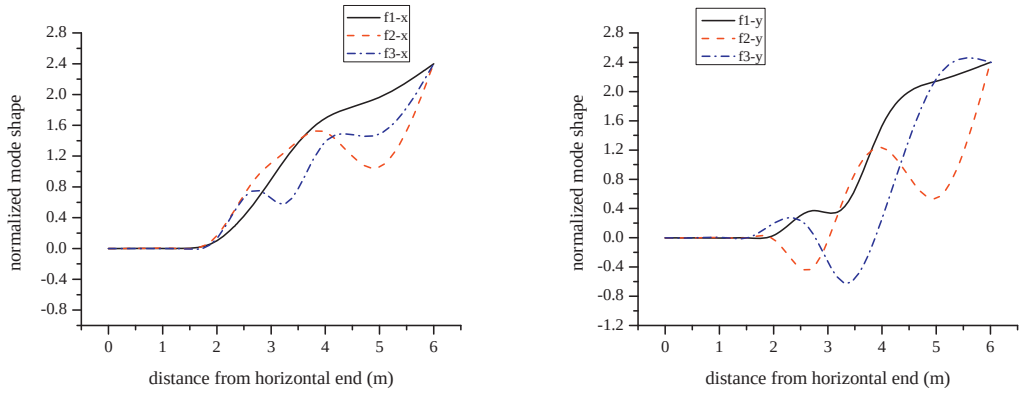

(a) Transversely (b) Vertically

Fig. 11. First three order mode shapes transversely and vertically.

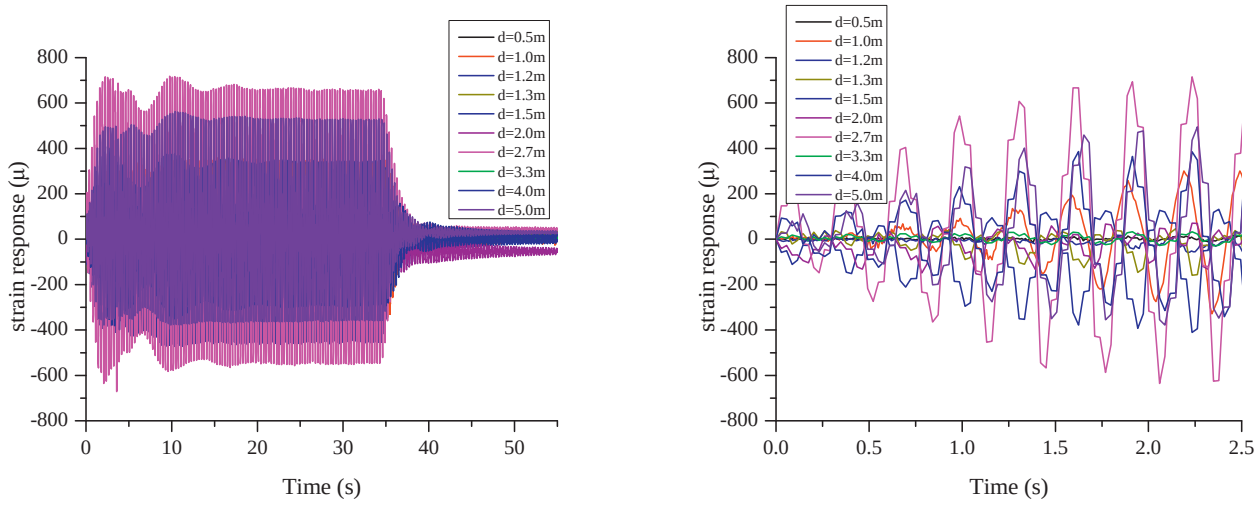

(a) Time history of whole process (b) Detail with enlarged time scale

Fig. 12. Time history of strain results from test.

was becoming free hanging during the earthquake. In contrast to the middle segment of TDZ, strain response in this section, shown in Fig. 13(d), is mainly assisted by compression, like an upward comb. This phenomenon shows that the soil suction holds the riser to the seabed, denoting the development of suction force at the pipe/soil interface.

Section $d = 2.7$ m – A position closest to the nominal TDP, which is not affected by the seabed, shows the greatest strain response, up to 718 micro-strain, as shown in Fig. 13(e). It located in the transition segment from TDZ to the catenary zone, as it was close to the seabed but not in contact with the seabed soil, it had to vibrate in the absence of constraints from seabed. Naturally, when the pipe–soil system was subjected to the earthquake, the seismic response in this position was most intense, becoming the most critical position.

Sections $d = 5.0$ m, this location is free hanging in the whole process of earthquake, representing the catenary zone of riser. It appeared the dynamic performance of a suspension structure. The strain response is essentially tension-compression symmetric, as shown in Fig. 13(f).

Fig. 14 shows the envelope of the strain response along pipeline. Overall, strain response of the pipeline along different positions is really complex. Strain response in TDZ is asymmetric, either assisted by tension or compression. And it is clear to see that there are two critical zone with large strain response, position near TDZ in catenary, and the position in catenary zone.

4.2.2. Strain response along pipe ring

In order to further study the strain response along pipe ring in some feature sections separately, Fig. 15 and Fig. 16 show time history of strains in section $d = 2.7$ m and section $d = 5.0$ m, respectively. Overall, as shown in Figs. 15(a) and Fig. 16(a), when the detected position located in the top end ($\psi = 0°$) and the bottom end ($\psi = 180°$) of a section, strain response ranged in a larger scope. Relatively, seismic response in side position ($\psi = 90°$) ranged in a really small scope. This phenomenon was revealed clearly in detailed figures with partial time scale in Figs. 15(b) and Fig. 16(b). Therefore, the critical position appeared on the top and bottom positions of

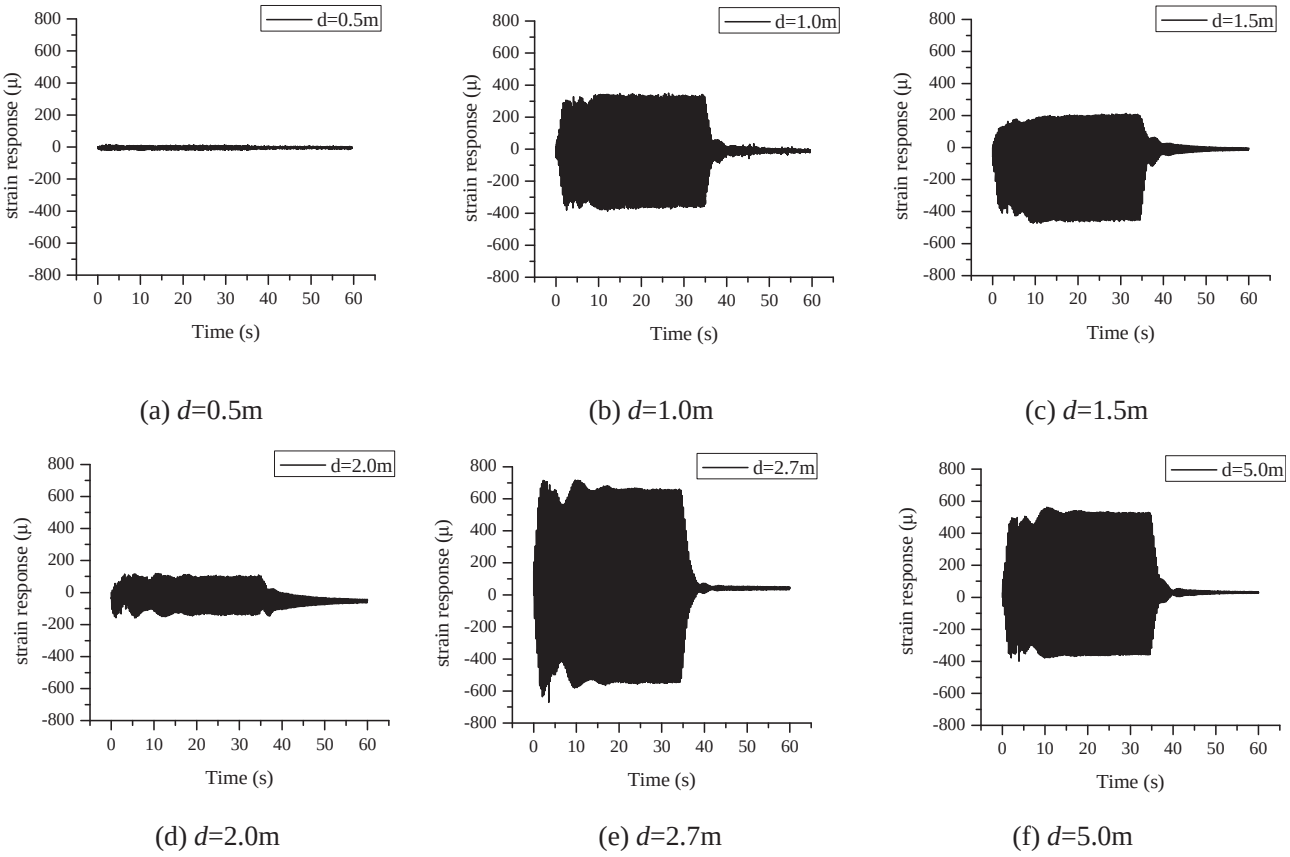

(a) d=0.5m (b) d=1.0m (c) d=1.5m

(d) d=2.0m (e) d=2.7m (f) d=5.0m

Fig. 13. Time history of strain under sinusoidal wave excitation.

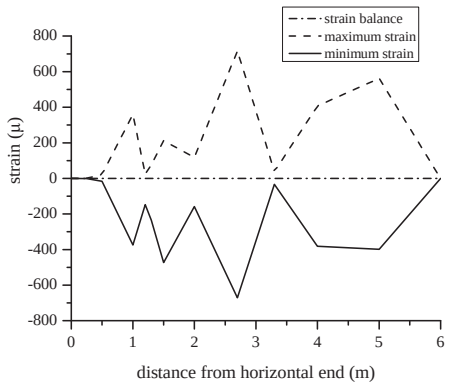

Fig. 14. Envelope of strain response under sinusoidal wave excitation.

pipeline. This study also shows When $\psi = 0°$, strain response in these two sections (solid lines in these figures) were basically symmetrical. This phenomenon was consistent with the analysis above. When $\psi = 180°$, the results in these two sections (dash dot lines) were asymmetric. This indicates that pipe soil interaction made greater impact on the lower part of the pipeline.

4.3. Random wave excitation

Pipe–soil system has also been subjected to random seismic wave, El-centro wave, whose peak acceleration is the same as the sinusoidal wave, a = 0.1 g. Compared to the artificial sinusoidal wave, whose excitation frequency (f = 3.32 Hz) was near the fundamental frequency of the system, the amplitude of strain response in section $d = 2.7$ m was much smaller than the strain response under artificial sinusoidal wave, as shown in Fig. 17(a). The peak values of the strain response of the riser under random and artificial earthquake waves are 91.65 and 681.94 micro-strain, respectively. Fig. 17(b) gives the comparison of frequency spectrum of strain responses under different waveforms. It shows that both the spectrums of strain response under different waveform excitation focused in a small range, around the fundamental frequency of riser, f = 3.32 Hz. The response is very small when the frequency is greater than 4.0 Hz or smaller than 2.0 Hz. However, when the system was subjected to different waveform, the peak of spectral response is very different. The peak of spectral response in section $d = 2.7$ m under random wave was 0.6 micro-strain, while the peak value under artificial earthquake was up to 40 micro-strain. This suggests the artificial excitation frequency satisfied the resonance condition, inducing the largest strain response amplitude.

4.4. Peak ground acceleration (PGA)

Fig. 18 shows the result of strain response in section $d = 2.7$ m under different peak ground acceleration. It can be seen that the shapes of time–history curves under different

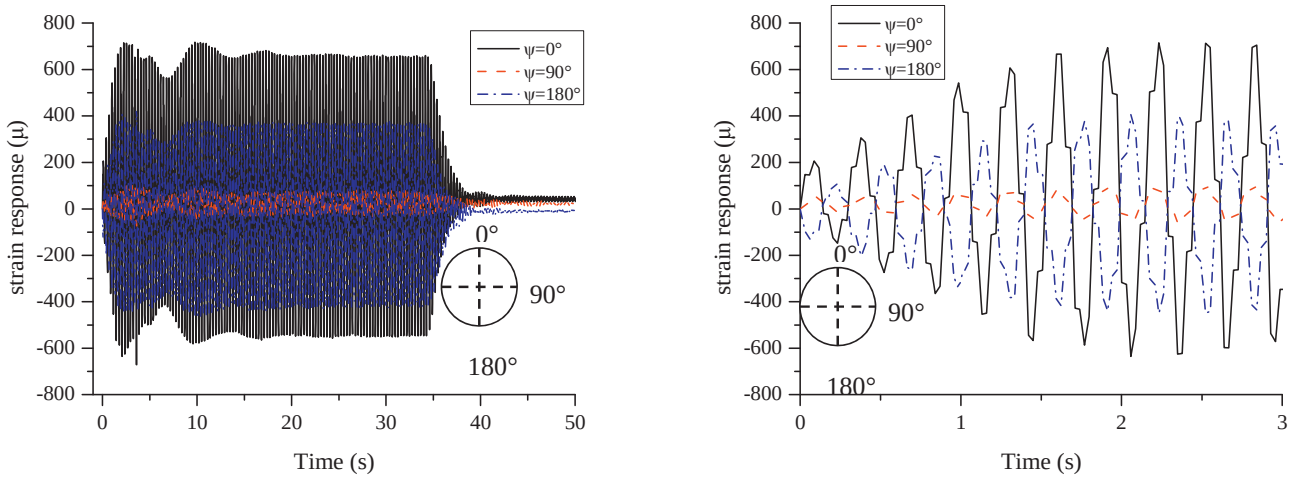

(a) Strain response along pipe ring (b) Detail with enlarged time scale

Fig. 15. Strain response along pipe ring in section $d = 2.7$ m.

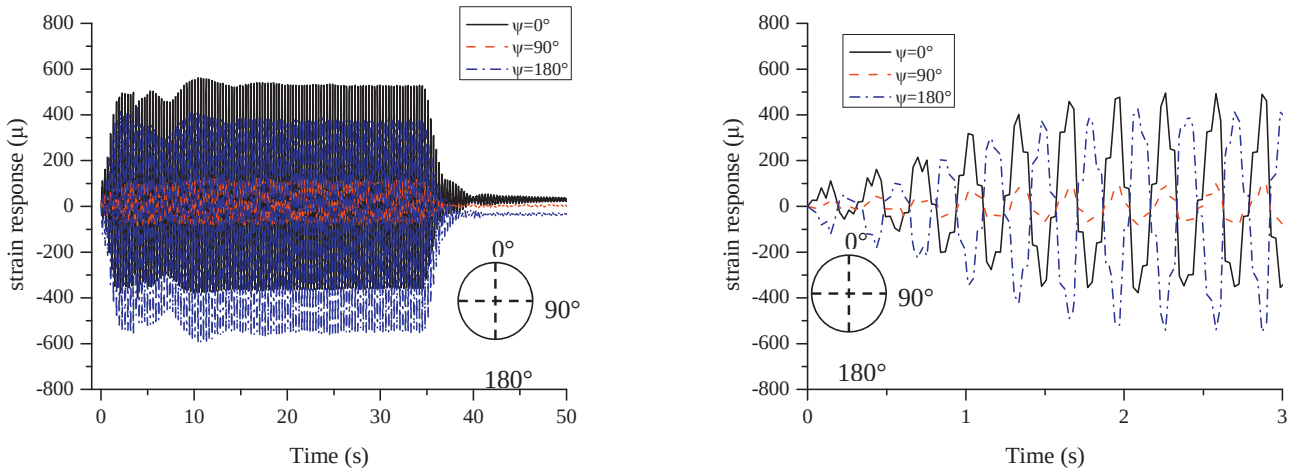

(a) Strain response along pipe ring (b) Detail with enlarged time scale

Fig. 16. Strain response along pipe ring in section $d = 5.0$ m.

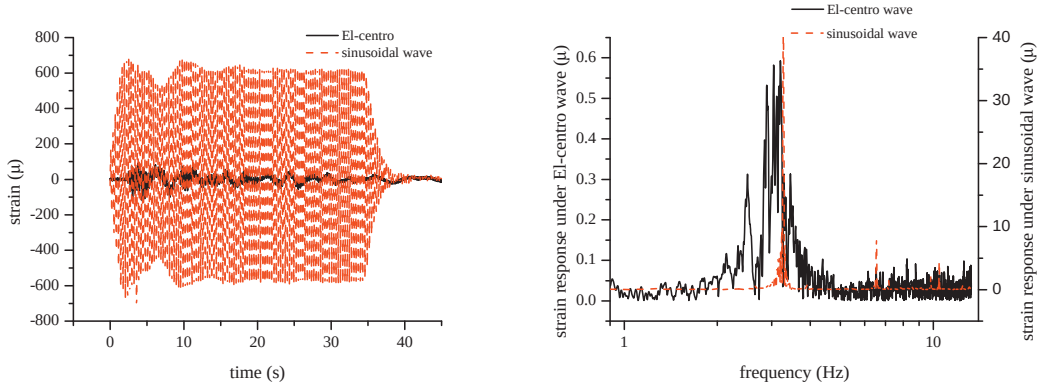

(a) Time history of strain response (b) Frequency spectrum of strain response

Fig. 17. Comparison of strain response under different waveform.

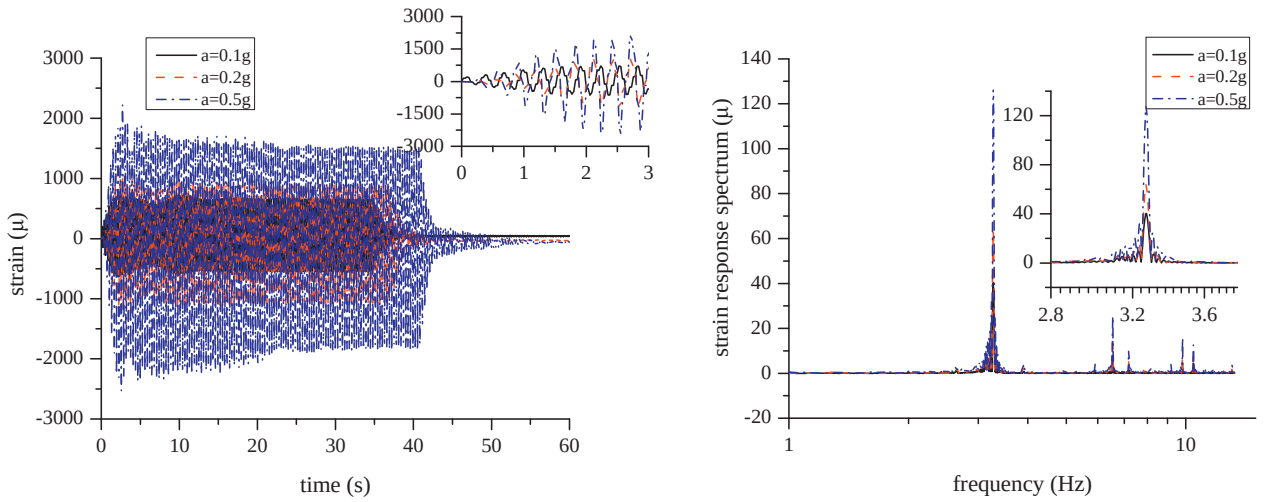

(a) Time history of strain response

(b) Frequency spectrum of strain response

Fig. 18. Comparison of strain response under different PGA.

earthquake amplitude are similar shown in Fig. 18(a). But the maximum strain responses of the riser were significantly increased from 717.3 to 1036.7, to 2225.3 micro-strain, with the increase of the excitation amplitude. So it can be expected that the riser in TDZ becomes much more dangerous due to the strengthened earthquake. Of course, the characteristic of frequency spectrums of strain response are also similar as shown in Fig. 18(b). The peak values of strain response spectrum increased with the increase of excitation amplitude. The peak values of strain response spectrum are 40.3, 64.0 and 127.8 micro-strain, respectively. Thus, the PGA is another most important parameter in seismic response of the riser in TDZ.

5. Conclusion

This paper describes a series of lab-scale indoor tests (modal test and seismic test) on a large-sized shaking table in DLUT. The first three order mode shapes and natural frequencies are obtained from the modal test. The seismic loading imposed on the bottom of the artificial seabed included artificial sinusoidal wave excitation and random El-centro earthquake excitation with different PGA. Seismic response of some feature points along pipeline and pipe ring was observed. Some other parameters of the seismic loading were also examined. Based on the test data, some valuable conclusions have been obtained:

(1) Mode shapes of the riser vertically and horizontally are basically the same except some difference around TDZ. But the absolute values of the natural frequency vertically are all higher than those corresponding values in transverse. It turned out that the geometry configuration of riser in TDZ affects its stiffness.
(2) As the seismic loading progressed, “beat” phenomenon appeared during the initiation of sinusoidal waveform loading, then the response trend to a stable state. And seabed soil deformed and its performance degenerated during the earthquake, the deformation of soil brought about the changes of pipe penetration and configuration, resulting different degrees permanent strain along pipeline.
(3) Overall, seismic response along pipeline presented alternating large or small phenomenon. During the earthquake, strain response in the surface zone was very small as pipeline there was constrained by the seabed. Pipeline in TDZ was subjected to alternating resistance or suction from seabed, so seismic response of strain there was asymmetric, In fact, a position near TDZ in catenary zone, $d = 2.7$ m, performed the maximum strain response, and a position almost in the middle of catenary zone, $d = 5.0$ m, becoming two critical zone with large strain response.
(4) Dynamic response presented a great difference along pipe ring, strain responses were severe when $\psi = 0°$ and $\psi = 180°$. It's relatively safe when $\psi = 90°$. The critical position appeared on the top and bottom positions of pipeline. Furthermore, strain response on the bottom section is showing significant asymmetry. That means pipe soil interaction made greater effect on the bottom of pipeline than the top of pipeline.
(5) Dynamic response of pipeline depends significantly on the waveform, and peak ground acceleration (PGA). Seismic response increased with the raise of PGA almost in the same magnitude. So it is important to investigate the geological conditions beforehand. The seismic response under sinusoidal wave was more intense than the random earthquake with the same excitation amplitude. So it is relatively conservative to calibrate structural performance by harmonic wave instead of random wave in the riser structure design.

Acknowledgements

The authors gratefully acknowledge the financial supports provided by National Program on Key Basic Research Project of China (973 Program) “whole-life service security of the

offshore structure in deep-sea extreme environment" [2011CB013702].

References

Arifin, R.B., Zhao, P., WMSBWM, Y., Bai, Y., 2010. Seismic Analysis for the Subsea Pipeline System. In: Proceedings of the ASME 2010 29th International Conference on Ocean. Offshore and Arctic Engineering, Shanghai, China, pp. 659−667.

Bai, X.L., Huang, W.P., Vaz, M.A., Yang, C.F., Duan, M.L., 2015. Riser-soil interaction model effects on the dynamic behavior of a steel catenary riser. Mar. Struct. 41, 53−76.

Bridge, C., Howells, H., Toy, N., Parke, G.A.R., Woods, R., 2003. Full scale model tests of a steel catenary riser. WIT Trans. Built Environ. 71, 107−116.

Dai, Y.Y., Zhou, J., 2016. Dynamic response of pipeline in touchdown zone under complicated loadings. In: Proceedings of the Twelfth Pacific-Asia Offshore Mechanics Symposium Gold Coast. ISOPE, Australia, pp. 419−424.

Duan, M.L., Wang, Y., Yue, Z.Y., Estenfen, S., 2010. Dynamics of risers for earthquake resistant designs. Petrol. Sci. 7 (2), 273−282.

Elosta, H., Huang, S., Incecik, A., 2013. Dynamic response of steel catenary riser using a seabed interaction under random loads. Ocean. Eng. 69, 34−43.

Firoozabad, E.S., Jeon, B.G., Choi, H.S., Kim, N.S., 2016. Failure criterion for steel pipe elbows under cyclic loading. Eng. Fail. Anal. 66, 515−525.

Hawlader, B., Dutta, S., Fouzder, S., Zakeri, A., 2015. Penetration of steel catenary riser in soft clay seabed: finite-element and finite-volume methods. Int. J. Geomech. 15, 04015008.

Hawlader, B., Fouzder, A., Dutta, S., 2016. Numerical modeling of suction and trench formation at the touchdown zone of steel catenary riser. Int. J. Geomech. 16, 04015033.

Hejazi, R., Kimiaei, M., 2016. Equivalent linear soil stiffness in fatigue design of steel catenary risers. Ocean. Eng. 111, 493−507.

Hodder, M.S., Byrne, B.W., 2010. 3D experiments investigating the interaction of a model SCR with the seabed. Appl. Ocean Res. 32 (2), 146−157.

Kim, Y.T., Kim, D.K., Choi, H.S., Yu, S.Y., Park, K.S., 2017. Fatigue performance of deepwater steel catenary riser considering nonlinear soil effect. Struct. Eng. Mech. 61 (6), 737−746.

Madani, B., Behnamfar, F., Tajmir, R.H., 2015. Dynamic response of structures subjected to pounding and structure-soil-structure interaction. Soil Dyn. Earthq. Eng. 78, 46−60.

Merifield, R.S., White, D.J., Randolph, M.F., 2009. Effect of surface heave on response of partially embedded pipelines on clay. J. Geotechnical Geoenvironmental Eng. 135, 819−829.

Park, K.S., Kim, Y.T., Kim, D.K., Yu, S.Y., Choi, H.S., 2016. A new method for strake configuration design of steel catenary riser. Ships Offshore Struct. 11 (4), 385−404.

Quéau, L.M., Kimiaei, M., Randolph, M.F., 2014. Analytical estimation of static stress range in oscillating steel catenary risers at touchdown areas and its application with dynamic amplification factors. Ocean. Eng. 88, 63−80.

Quéau, L.M., Kimiaei, M., Randolph, M.F., 2015a. Approximation of the maximum dynamic stress range in steel catenary risers using artificial neural networks. Eng. Struct. 92, 172−185.

Quéau, L.M., Kimiaei, M., Randolph, M.F., 2015b. Sensitivity studies of SCR fatigue damage in the touchdown zone using an efficient simplified framework for stress range evaluation. Ocean. Eng. 96, 295−311.

Ryu, D.M., Lee, C., Lee, C.S., Choi, K.H., Koo, B.Y., Song, J.K., Kim, M.H., Lee, J.M., 2015. Lab-scale impact test to investigate the pipe-soil interaction and comparative study to evaluate structural responses. Int. J. Nav. Archit. Ocean Eng. 7 (4), 720−738.

Wang, K.P., Xue, H.X., Tang, W.Y., Guo, J.T., 2013. Fatigue analysis of steel catenary riser at the touch-down point based on linear hysteretic riser-soil interaction model. Ocean. Eng. 68, 102−111.

Wang, L.Z., Zhang, J., Yuan, F., Li, K., 2014. Interaction between catenary riser and soft seabed: large-scale indoor tests. Appl. Ocean Res. 45, 10−21.

Won, J.H., Mha, H.S., Kim, S.H., 2015. Effects of the earthquake-induced pounding upon pier motions in the multi-span simply supported steel girder bridge. Eng. Struct. 93, 1−12.

Wu, Z.W., Liu, J.K., Lu, Z.R., 2016. Parametrically excited vibrations of marine riser under random wave forces and earthquake. Adv. Struct. Eng. 19 (3), 449−462.

Yu, S.Y., Choi, H.S., Lee, S.K., Do, C.H., Kim, D.K., 2013. An optimum design of on-bottom stability of offshore pipelines on soft clay. Int. J. Nav. Archit. Ocean Eng. 5 (4), 598−613.

Yu, S.Y., Choi, H.S., Lee, S.K., Park, K.S., Kim, D.K., 2015. Nonlinear soil parameter effects on dynamic embedment of offshore pipeline on soft clay. Int. J. Nav. Archit. Ocean Eng. 7 (2), 227−243.

Yu, S.Y., Choi, H.S., Park, K.S., Kim, Y.T., Kim, D.K., 2017. Advanced procedure for estimation of pipeline embedment on soft clayed seabed. Struct. Eng. Mech. 62 (4), 381−389.

Zheng, Z.C., Chen, J.R., Zhu, Z.Y., 2004. Physical and mechanical characteristics of seabed soils and its geological environment in South China Sea. Hydrogeol. Eng. Geol. 4, 50−53, 65.